Chapter 5

GRID-CONTROLLED TUBES— STATIC CHARACTERISTICS

If a grid is placed in front of a thermionically emitting cathode and if the current drawn from the cathode is space-charge-limited, the voltage applied to the grid can be used to control the current drawn from the cathode. A triode vacuum tube consists of a cathode, a control grid, and an anode. Usually, a dc bias voltage is applied to the control grid to make it negative with respect to the potential minimum and thereby reduce the interception of the electron beam by the grid. By superimposing a small ac signal on the dc bias voltage, the beam current can be modulated with little expenditure of power. AC power amplification is then obtained by causing the ac current flowing in the anode circuit to pass through a load resistance or impedance of suitable size.

Additional grids also may be inserted between the control grid and anode. Generally, these are held at fixed potentials, but in some cases their control action on the beam is used to mix signals from independent sources. A tetrode has a control grid and a screen grid, whereas a pentode has a control grid, a screen grid, and a suppressor grid.

Usually the screen grid in a tetrode is biased at a fixed positive potential with respect to the cathode. Its shielding action between the anode and control grid reduces the capacitance between these electrodes and hence the coupling between the output circuit and the input circuit. In addition, the current reaching the anode of a tetrode is determined largely by the voltages applied to the control grid and screen grid and is nearly independent of anode voltage over a wide range of positive anode voltages. This is an advantage when high-voltage amplification per stage is required.

Many tetrodes are constructed with a large spacing between the screen grid and anode so that space charge in the interelectrode space will depress the potential between the electrodes and prevent secondary electrons

emitted from one electrode from reaching the other. The large spacing also reduces the output capacitance of the tube, and this is an advantage in high-gain, broadband amplifiers.

In the pentode, the supressor grid is inserted between the screen grid and anode. It is of a very coarse mesh, and usually it is biased at cathode potential. The suppressor grid depresses the potential between the screen grid and anode and thereby prevents secondary-electron exchange between these electrodes.

In the present chapter we consider the dc behavior of triodes, tetrodes, and pentodes. The mechanical construction and performance of one example of each of these tubes is described. In Chapter 6 the use of grid-controlled tubes in simple low-frequency amplifier circuits is described, and in Chapter 7 the problems and limitations of grid-controlled tubes when operated at very high frequencies are discussed.

As in the previous chapter, we shall use the subscript o to designate dc electrode voltages and currents. Thus V_{ao} and I_{ao} are the dc anode voltage and current.

5.1 A Particular Triode and its Electric Field in the Absence of Space Charge

In this section we first describe the electrode geometry and construction of a particular triode, the Western Electric 417A. Then we consider the electric fields in the interelectrode space of this tube when various potentials are applied to the electrodes, and when no space charge is present. The electrical characteristics of the 417A with space-charge-limited operation are described in Section 5.2.

The construction of the 417A is shown in Figure 5.1-1. This is an example of a triode in which the grid is mounted very close to the cathode to increase the effectiveness of the grid voltage in controlling the current reaching the anode. The tube is used in the input stage[1] of a broadband amplifier which amplifies signals with frequencies varying from 58 to 90 Mc/sec.

Table 5.1-1 summarizes the important dimensions of the 417A electrodes. The cathode area is 0.38 cm^2.

The cathode consists of a short length of nickel tubing that is flattened to provide two planar emitting surfaces. The wall thickness of the tubing is

[1]Actually two tubes are used in a "cascode" stage. Triodes are preferred for the input stages of high-gain amplifiers because they generate less noise than tetrodes and pentodes. Since the noise generated by the input stages is amplified by all the remaining stages, the noise output of a high-gain amplifier is much reduced by using low-noise tubes in the input stages.

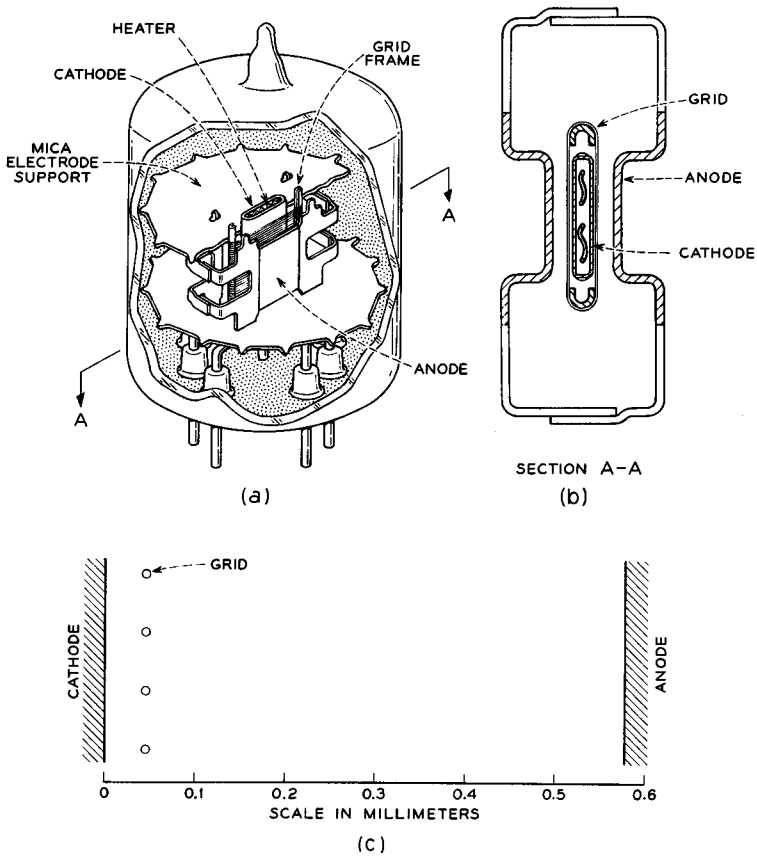

FIG. 5.1-1 The construction of the Western Electric 417A triode. The overall height of the tube is 4.4 cm.

TABLE 5.1-1

	Millimeters
Grid wire diameter	0.0074 (or 0.00029 inch)
Grid pitch, P (or center-to-center spacing of the grid wires)	0.065
Cathode-to-grid spacing, d_{cg}	0.045
Cathode-to-anode spacing, d_{ca}	0.58

0.075 mm. A "double-carbonate" oxide coating is applied to the emitting surfaces.

The grid is made by winding tungsten wire onto a molybdenum frame and then brazing the wire to the frame with a small amount of gold. The high

tensile strength of tungsten permits winding the grid wire onto the molybdenum frame while it is under appreciable tension.[2] This ensures that the resonant frequency of the grid wires is high and minimizes the tendency for mechanical excitation when the tube is vibrated. Vibration of grid wires in grid-controlled tubes is a principal source of "microphonics." After brazing the grid wires to the frame, the grid assembly is gold plated to raise its work function. This reduces thermionic emission from the grid wires, which would otherwise take place when the grid is heated by thermal radiation from the cathode.[3]

The anode, or "plate," of the 417A is made of nickel which is coated with fine carbon particles in order to increase the heat radiation from the outer surface and thereby reduce the anode operating temperature. Under typical operating conditions, a power of 3.5 watts is dissipated in the anode, and the anode temperature is between 500° and 600°C.

Let us consider now the potential obtained in the interelectrode space of the 417A when various voltages are applied to the electrodes and when no space charge is present. It is convenient to think of the potential as being a linear combination of two separate potential functions, which we shall denote $F_1(x,y,z)$ and $F_2(x,y,z)$. $F_1(x,y,z)$ is the potential obtained in the interelectrode space when the grid is at +1 volt, and the cathode and anode are at ground potential. $F_2(x,y,z)$ is the potential obtained when the anode is at +1 volt and the grid and cathode are grounded. Clearly the functions F_1 and F_2 satisfy Laplace's Equation, and so does any linear combination of them. In particular, the linear combination given by $V(x,y,z) = V_{go}F_1 + V_{ao}F_2$ satisfies the boundary conditions for the case in which the cathode is at ground potential, and the grid and anode are at V_{go} and V_{ao} volts, respectively. Since it also satisfies Laplace's Equation, it must be the potential function actually obtained with these boundary conditions.

Let us look more closely now at the functions F_1 and F_2. Figure 5.1-2(a) shows a plot of equipotential contours of the function F_1 in a portion of the interelectrode space of the 417A.[4] Figure 5.1-2(b) shows plots of F_1 along two lines running from the cathode to the anode; one line passes through the center of a grid wire, and the other passes midway between grid wires. Figures 5.1-2(c) and (d) show similar plots for the function F_2.

---

[2]About half the breaking tension of the tungsten wire is used.

[3]Grid emission tends to bias the grid in the positive direction. This increases the beam current and the power dissipation in the tube, which in turn raises the grid operating temperature and further aggravates the situation. In an extreme case, with a very high resistance in the grid circuit, a tube with high grid emission can be destroyed by excessive power dissipation in its electrodes.

[4]Plots such as this can be made with the aid of an electrolytic tank. See, for instance, Reference 4a, p. 180. Analytic expressions for F_1 and F_2 are given in Reference 5.1, Equations 1 to 4. Approximate expressions are derived in Appendix IX.

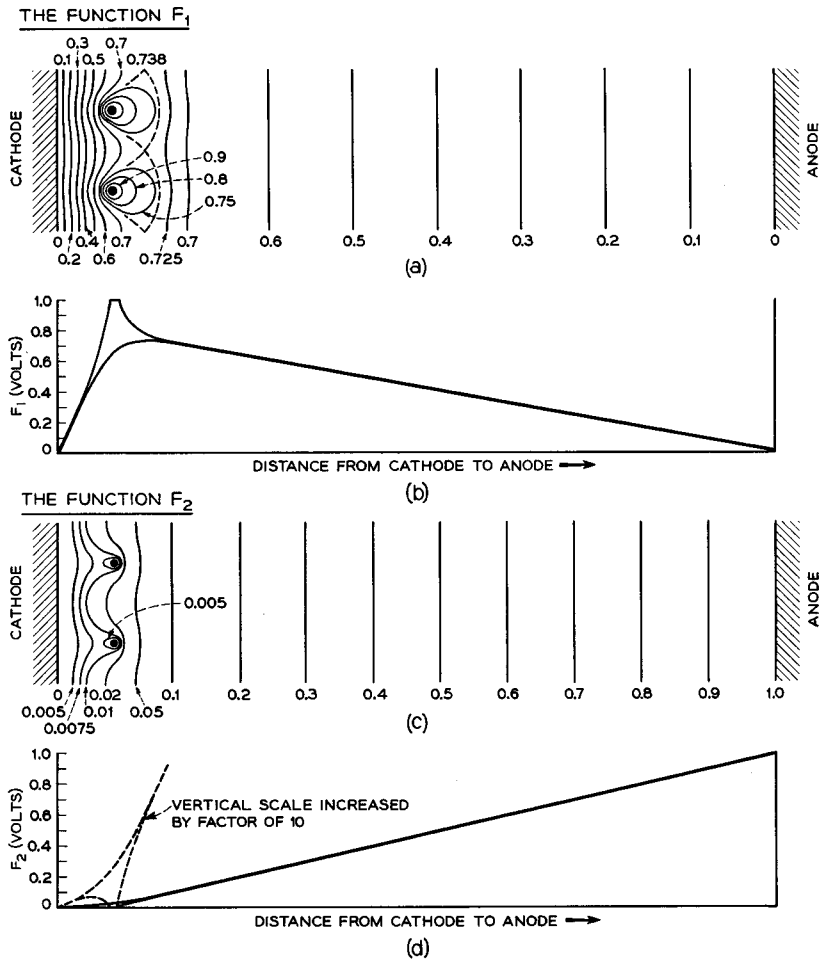

FIG. 5.1-2 Plots of the functions F_1 and F_2 for the interelectrode space of the 417A.

At the cathode the function F_1 has a slope of 176 volts/cm for the 417A, whereas the function F_2 has a slope of 3.8 volts/cm. The ratio of these electric fields is called the electrostatic amplification factor and is designated μ_{es}. Thus

$$\mu_{es} = \frac{\left.\frac{\partial F_1}{\partial x}\right|_{x=0}}{\left.\frac{\partial F_2}{\partial x}\right|_{x=0}} \tag{5.1-1}$$

where x measures distance in the direction normal to the cathode and is zero at the cathode. For the 417A, $\mu_{es} = 176/3.8 = 46$.

The electrostatic amplification factor measures the relative effectiveness of the grid and anode in creating an electric field at the cathode surface. In fact, a second definition of μ_{es} which follows directly from Equation (5.1-1) is that μ_{es} is minus the ratio of the anode voltage to grid voltage which gives zero electric field at the cathode. Finally, since electric fields can be superposed, we can write

$$\mu_{es} = -\left.\frac{dV_{ao}}{dV_{go}}\right|_{\text{constant electric field at the cathode}} \tag{5.1-2}$$

where dV_{ao} and dV_{go} are incremental changes in the anode and grid voltages which give zero change in the electric field at the cathode.

Figure 5.1-3 shows plots of $V = V_{go}F_1 + V_{ao}F_2$ in the region of the cathode and grid of the 417A for an anode voltage of 100 volts and three values of V_{go}. For the particular geometry of this tube, a grid voltage of -2.2 volts gives nearly zero electric field at the cathode. Using the second definition of the electrostatic amplification factor, given above, we find that $\mu_{es} = 100/2.2 = 45.5$, or approximately 46, in agreement with the value previously obtained using Equation (5.1-1). If the grid voltage is changed by 1 volt with constant anode voltage, the electric field at the cathode surface changes by

$$\left.\frac{\partial F_1}{\partial x}\right|_{x=0} = 176 \text{ volts/cm}$$

Thus, we can expect that the control action of the grid voltage upon the current drawn from the cathode with space-charge-limited operation will be considerable.

From the foregoing discussion it is evident that the electrostatic amplification factor is entirely a function of the geometry of the electrodes. In Appendix IX it is shown that an approximate expression for the electrostatic amplification factor of a planar triode is given by

$$\mu_{es} = -\frac{2\pi d_{ga}}{P \ln\left(2 \sin \frac{\pi R}{P}\right)} \tag{5.1-3}$$

where d_{ga} is the grid-to-anode distance, P is the grid pitch, and R is the grid-wire radius. The expression is valid when the cathode-to-grid spacing $d_{cg} \geq P$ and when $R \leq P/20$. The electrostatic amplification factor is independent of the area of the electrodes, but it increases as the grid-to-anode distance is increased. It also increases if the grid-wire radius and grid pitch are decreased in such a manner that the ratio of wire radius to

FIG. 5.1-3 Plots of $V = V_{go}F_1 + V_{ao}F_2$ in the region of the cathode and grid of the 417A for $V_{ao} = 100$ volts and $V_{go} = -3.4$, -2.2, and -1.0 volts.

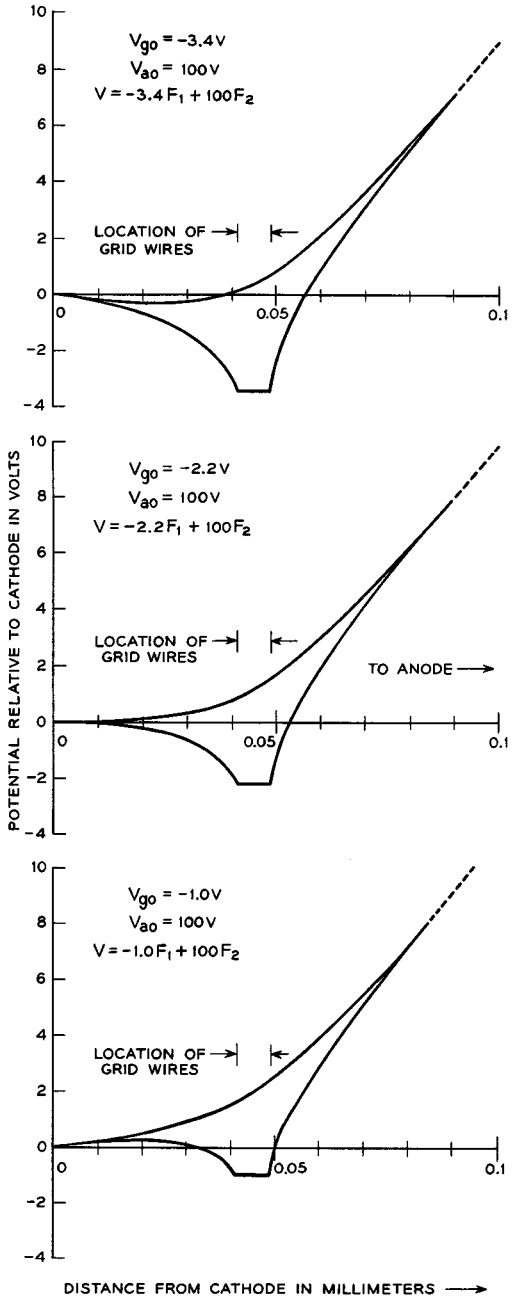
$V_{go} = -3.4V$
$V_{ao} = 100V$
$V = -3.4F_1 + 100F_2$
LOCATION OF GRID WIRES
$V_{go} = -2.2V$
$V_{ao} = 100V$
$V = -2.2F_1 + 100F_2$
LOCATION OF GRID WIRES
TO ANODE
$V_{go} = -1.0V$
$V_{ao} = 100V$
$V = -1.0F_1 + 100F_2$
LOCATION OF GRID WIRES
10
8
6
4
2
0
-2
-4
0
0.05
0.1
POTENTIAL RELATIVE TO CATHODE IN VOLTS
DISTANCE FROM CATHODE IN MILLIMETERS

pitch is maintained constant. (The ratio $2R/P$ is sometimes called the *screening fraction* of the grid because it indicates the fraction of the electrode area which is screened or shadowed by the grid.) Note that Equation (5.1-3) indicates that μ_{es} is independent of the cathode-to-grid spacing. Also given in Appendix IX are expressions for the functions F_1 and F_2 which are valid when $d_{cg} \geq P$ and when $R \leq P/20$.

Since $V = V_{go}F_1 + V_{ao}F_2$, we can express the gradient of potential in the x direction as

$$\frac{\partial V}{\partial x} = V_{go}\frac{\partial F_1}{\partial x} + V_{ao}\frac{\partial F_2}{\partial x}$$

$$= \frac{\partial F_1}{\partial x}\left(V_{go} + V_{ao}\frac{\frac{\partial F_2}{\partial x}}{\frac{\partial F_1}{\partial x}}\right) \tag{5.1-4}$$

At the cathode, the potential gradient is therefore given by

$$\left.\frac{\partial V}{\partial x}\right|_{x=0} = \left.\frac{\partial F_1}{\partial x}\right|_{x=0}\left(V_{go} + \frac{V_{ao}}{\mu_{es}}\right) \tag{5.1-5}$$

Thus the off-cathode field in the absence of space charge is proportional to the voltage $(V_{go} + V_{ao}/\mu_{es})$. We shall find in the next section that the electrical behavior of a triode in the presence of space charge is dependent upon a voltage which is very nearly equal to $(V_{go} + V_{ao}/\mu_{es})$.

5.2 The Triode with Space Charge

Grid-controlled tubes are almost always operated with the current drawn from the cathode space-charge-limited since only then is it possible for the grid to act effectively as a control electrode. If the cathode emission were ideally temperature-limited, the current drawn from the cathode would be independent of the grid voltage for all grid voltages at which temperature-limited emission prevailed.

Figure 5.2-1 shows the grid and anode "characteristic curves" for the 417A triode. These curves give the relationship between the current reaching the anode and the voltages applied to the grid and anode. The grid of the 417A is generally "biased" negatively with respect to the potential minimum to prevent it from intercepting the electron beam.

The circuit designer is frequently concerned with the small-signal behavior of the active devices in his circuits and consequently with the slopes of the curves relating the currents reaching the terminals of a device to the voltages applied between the terminals. In the case of the triode, the small-signal behavior of the tube can be described in terms of the slopes of the

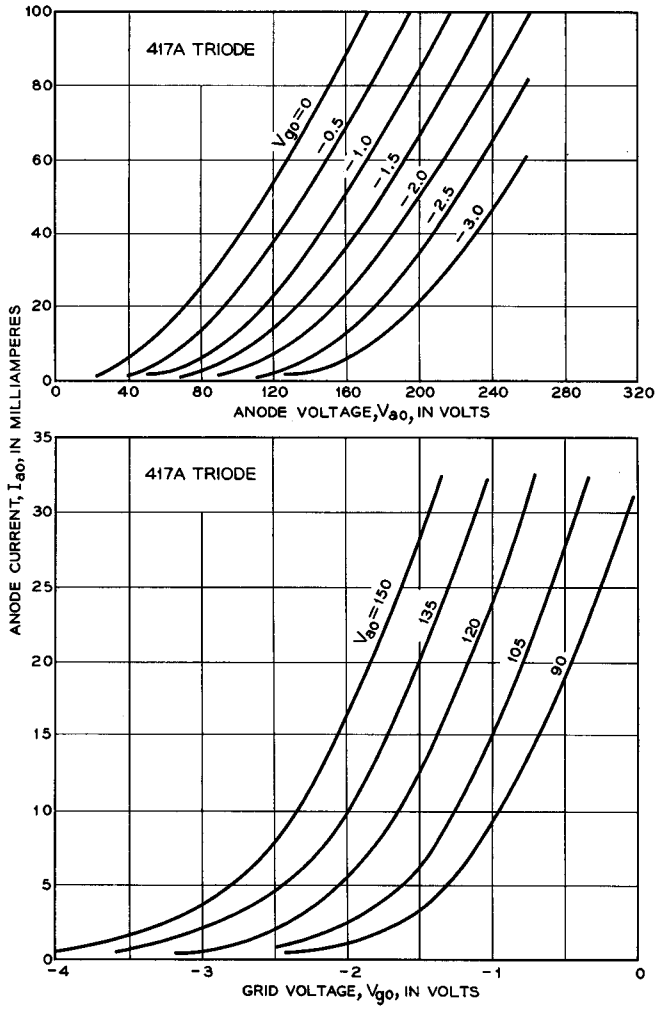

FIG. 5.2-1 The grid and anode characteristic curves for the 417A triode.

characteristic curves. Two parameters which are derived from these slopes are the transconductance and the dynamic anode resistance, or dynamic plate resistance. The transconductance is denoted by[5] g_m and is defined as

$$g_m = \frac{dI_{ao}}{dV_{go}}\bigg|_{V_{ao}} = \frac{\partial I_{ao}}{\partial V_{go}} \tag{5.2-1}$$

[5]Sometimes by S_m.

where I_{ao} is the dc anode current. The dynamic anode resistance, denoted by r_a, is defined as

$$r_a = \frac{dV_{ao}}{dI_{ao}}\bigg|_{V_{go}} = \frac{\partial V_{ao}}{\partial I_{ao}} \tag{5.2-2}$$

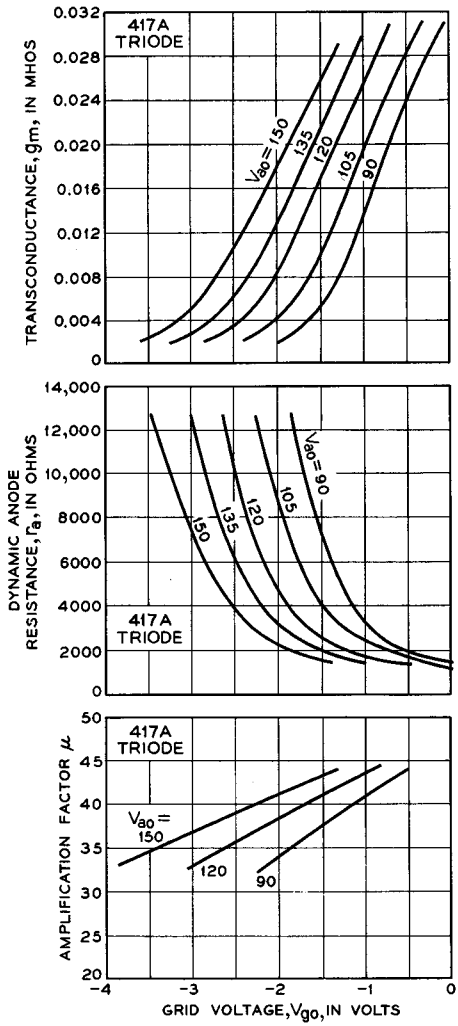

FIG. 5.2-2 The transconductance, the dynamic anode resistance, and the amplification factor of the 417A triode as a function of the grid voltage and anode voltage.

The product of g_m and r_a is called the *amplification factor* and is denoted by μ. Thus

$$\mu = g_m r_a \tag{5.2-3}$$

The amplification factor also can be expressed in differential form, similar to the expressions given above for g_m and r_a. Suppose that V_{go} and V_{ao} undergo differential changes dV_{go} and dV_{ao} at a time when the tube is drawing anode current I_{ao}. The resulting change in anode current is given by

$$\begin{aligned} dI_{ao} &= \frac{\partial I_{ao}}{\partial V_{go}} dV_{go} + \frac{\partial I_{ao}}{\partial V_{ao}} dV_{ao} \\ &= g_m dV_{go} + \frac{1}{r_a} dV_{ao} \end{aligned} \tag{5.2-4}$$

Now if dV_{go} and dV_{ao} are such that $dI_{ao} = 0$, then

$$g_m r_a = -\frac{dV_{ao}}{dV_{go}}\bigg|_{I_{ao}} \tag{5.2-5}$$

and hence

$$\mu = -\frac{dV_{ao}}{dV_{go}}\bigg|_{I_{ao}} \tag{5.2-6}$$

The amplification factor μ is usually approximately equal to the electrostatic amplification factor μ_{es}. Comparison of Equations (5.1-2) and (5.2-6) makes this approximate equality seem reasonable.

Figure 5.2-2 shows plots of the transconductance, the dynamic anode resistance, and the amplification factor of the 417A for various values of grid voltage and anode voltage. Evidently the transconductance increases with increasing anode current, the amplification factor is nearly independent of anode current, and the dynamic anode resistance decreases with increasing anode current. Typical operating conditions for the 417A are given in Table 5.2-1.

Consider the dependence of the anode current on the electrode potentials. It is found experimentally that an approximate expression for the current drawn to the anode of a triode is

$$I_{ao} = C\left(V_{go} + \frac{V_{ao}}{\mu}\right)^n \tag{5.2-7}$$

where C and n are constants. Values of n generally lie between 3/2 and 2, but in some cases may be as high as 5/2. The expression is found to hold even for small positive grid voltages, provided the anode voltage is much greater than the grid voltage. The dependence of the anode current upon the voltage $V_{go} + V_{ao}/\mu$ is perhaps not surprising, since we found in the last section that the off-cathode field in the absence of space charge is pro-

TABLE 5.2-I SOME CHARACTERISTICS OF TUBES DESCRIBED IN CHAPTERS 5 AND 7

		417A Triode	416B Triode	448A Tetrode	1983 Tetrode	350B Beam Power Tetrode	403A/6AK5 Pentode
(a)	Anode Voltage, volts	130	200	125	300	250	120
	Anode Current, milliamperes	27	30	25.5	40	62	7.5
	Anode Power, watts	3.5	6.0	3.2	12	15.5	0.9
(b)	Screen Grid Voltage, volts	–	–	125	200	250	120
	Screen Grid Current, milliamperes	–	–	9.0	5	7	2.5
	Screen Grid Power, watts	–	–	1.1	1.0	1.7	0.3
(c)	Control Grid Bias, volts	−1.2	−0.1	−1.1	−0.8	−18	−2.0
(d)	Transconductance g_m, micromhos	25,000	60,000	34,000	45,000	6,900	5,000
	Dynamic Anode Resistance r_a, ohms	1,700	5,000	32,000	–	18,000	300,000
	Amplification Factor μ	43	300	1100	–	124	1500
(e)	Cathode Area A, cm^2	0.38	0.164	0.86	0.164	3.6	0.18
	Cathode Current Density, milliamperes/cm^2	71	180	40	270	19	56
	Transconductance Per Unit Area of Cathode g_m/A, micromhos/cm^2	66,000	370,000	40,000	280,000	1,900	28,000
(f)	Cathode-Control Grid Spacing, millimeters	0.045	0.018	0.060	0.030	0.56	0.077
	Input Capacitance (Operating) C_i, pf	–	–	23	13.6	–	6.4
	Output Capacitance C_o, pf *	1.8	1.4	2.1	1.3	8.0	2.0
	Gain-Bandwidth Product With Single Tuned Circuit Between Stages $\frac{g_m}{2\pi(C_o+C_i)}$, megacycles	–	–	215	480	–	95
(g)	Cathode Lead Inductance, millimicrohenries	–	–	4	0.7	–	–

* 1 picofarad = 10^{-12} farad.

portional to $V_{go} + V_{ao}/\mu_{cs}$, and we have noted in the present section that $\mu \approx \mu_{cs}$.

In a triode in which the grid is well beyond the region of the potential minimum, the anode and grid combine to create a field on the grid side of the potential minimum which is approximately proportional to $V_{go} + V_{ao}/\mu$. For such a triode we would expect from the discussion given in Section 4.2 that a value of n equal to 3/2 would be applicable in Equation (5.2-7), and the anode current would vary as $(V_{go} + V_{ao}/\mu)^{3/2}$.

The constant C in Equation (5.2-7) can be evaluated for a planar triode in which $n = 3/2$ in the manner outlined below. Let us first assume that the grid is removed and the tube is operated as a space-charge-limited diode. From Equation (4.1-9) the current drawn to the anode would be

$$I_{ao} = 2.33 \times 10^{-6} \frac{V_{ao}^{3/2}}{d_{ca}^{2}} A \tag{5.2-8}$$

where d_{ca} is the distance from the potential minimum to the anode, and A is the cathode area. Solving for V_{ao}, we obtain

$$V_{ao} = \left[\frac{I_{ao}}{2.33 \times 10^{-6} A} \right]^{2/3} d_{ca}^{4/3} \tag{5.2-9}$$

Next let the grid be inserted at a distance d_{cg} from the potential minimum, and let the applied grid voltage be that which was present in the beam at the same location before the grid was inserted. A plot of the potential distribution between the potential minimum and the anode for these conditions is

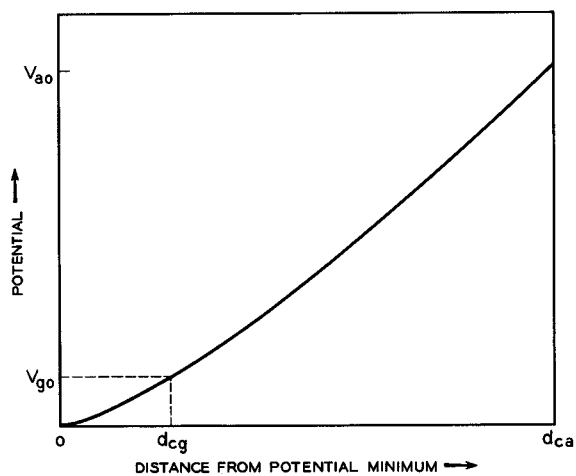

FIG. 5.2-3 The potential distribution in a space-charge-limited triode with the grid at beam potential.

shown in Figure 5.2-3. The applied grid voltage under these circumstances is given by

$$V_{go} = \left[\frac{I_{ao}}{2.33 \times 10^{-6} A}\right]^{2/3} d_{cg}^{4/3} \tag{5.2-10}$$

With the grid at the potential of the surrounding beam, some of the beam current is intercepted by the grid wires. However, if the grid-wire diameter is much smaller than the grid-wire spacing, this interception will be a small part of the total anode current.

Substituting the above expressions for V_{ao} and V_{go} into Equation (5.2-7) and setting $n = 3/2$, we obtain

$$I_{ao} = C\frac{I_{ao}}{2.33 \times 10^{-6} A}\left[d_{cg}^{4/3} + \frac{d_{ca}^{4/3}}{\mu}\right]^{3/2} \tag{5.2-11}$$

from which

$$C = \frac{2.33 \times 10^{-6} A}{\left[d_{cg}^{4/3} + \dfrac{d_{ca}^{4/3}}{\mu}\right]^{3/2}} \tag{5.2-12}$$

Finally, the anode current can be expressed as

$$I_{ao} = \frac{2.33 \times 10^{-6} A (V_{go} + V_{ao}/\mu)^{3/2}}{d_{cg}^{2}\left[1 + \dfrac{1}{\mu}\left(\dfrac{d_{ca}}{d_{cg}}\right)^{4/3}\right]^{3/2}} \tag{5.2-13}$$

This last equation states that the current density drawn from the cathode of a planar triode is the same as would be drawn by a planar diode having a cathode-to-anode distance of

$$d_{cg}\left[1 + \frac{1}{\mu}\left(\frac{d_{ca}}{d_{cg}}\right)^{4/3}\right]^{3/4}$$

and an applied anode voltage of $V_{go} + V_{ao}/\mu$. Replacing

$$d_{cg}\left[1 + \frac{1}{\mu}\left(\frac{d_{ca}}{d_{cg}}\right)^{4/3}\right]^{3/4}$$

by d_e, where d_e is called the equivalent diode spacing of the triode, Equation (5.2-13) becomes $I_{ao} = 2.33 \times 10^{-6} A\ (V_{go} + V_{ao}/\mu)^{3/2}/d_e^2$. The distance d_e is a function of the tube dimensions only; it is always greater than d_{cg} and frequently less than $2d_{cg}$.

As the grid is moved closer to the cathode, the potential $V_{go} + V_{ao}/\mu$ affects not only the electric field on the anode side of the potential minimum, but *it affects the potential at the minimum.* The dependence of the anode current upon the voltage $V_{go} + V_{ao}/\mu$ then increases, and accordingly the

exponent n in Equation (5.2-7) increases. For many "close-spaced" triodes, that is, triodes with small d_{cg}, n is more nearly equal to 2 than 3/2. Figure 5.2-4(a) shows a plot of I_{ao} vs. $(V_{go} + V_{ao}/\mu)$ for the 417A triode. From the figure it can be seen that a value of n equal to 2 is appropriate for

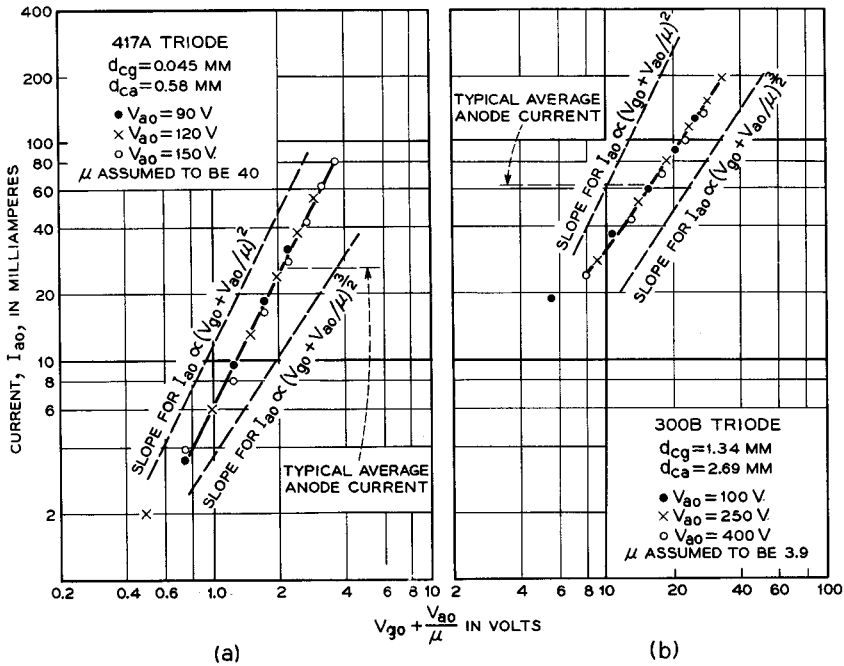

FIG. 5.2-4 Plots of I_{ao} vs. $(V_{go} + V_{ao}/\mu)$ for the 417A triode and the 300B triode.

this tube. Figure 5.2-4(b) shows a plot of I_{ao} vs. $(V_{go} + V_{ao}/\mu)$ for the Western Electric 300B triode in which the cathode-to-grid spacing is approximately half the cathode-to-anode spacing. Clearly, $n = 3/2$ is appropriate for this tube.

To determine the relative positions of the grid plane and the plane of the potential minimum in the 417A, we have plotted in Figure 5.2-5 the potential in a planar diode in which a current density of 0.071 amp/cm^2 passes the potential minimum.[6] Such a current density might be typical of that passing the potential minimum in the 417A. A cathode emission current density of 0.5 amp/cm^2 and a cathode temperature of 1025°K are assumed. The position of the grid wires in the 417A is shown in the figure. The plane

[6]The method for obtaining the potential plot is described in References 5.2 and 5.3.

of the grid wires is about three times as far from the cathode as the plane of the potential minimum. Of course, the potential on the grid side of the potential minimum in the 417A would be much different from that shown by the dashed curve in Figure 5.2-5, because the grid bias voltage depresses

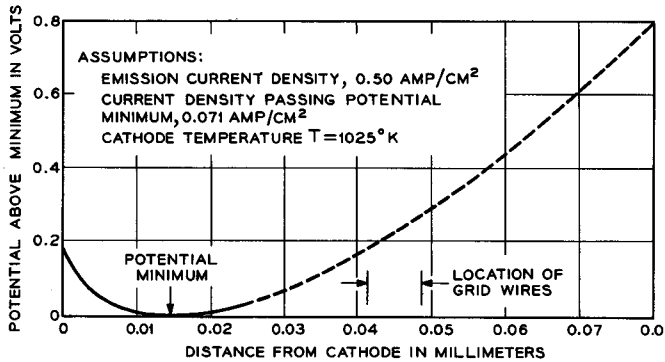

FIG. 5.2-5 The potential in a planar diode in which the current density passing the potential minimum is typical of that used in the 417A.

the potential in the region of the grid wires, and the potential midway between grid wires is much higher.

From Figure 5.1-3 it is evident that in the absence of space charge the potential over a plane which lies one third of the way out from the cathode to the grid wires is not uniform. Consequently, when space-charge-limited conditions prevail, we would expect the potential at the potential minimum would be slightly higher at points opposite the center of the opening between grid wires than directly under the grid wires. This means that the current passing the potential minimum is lower directly under the grid wires, and, if the grid voltage is made increasingly negative, the current passing the potential minimum will first cut off directly under the grid wires. This phenomenon is called *Inselbildung* or "island building." Some consequences of Inselbildung are described in Reference 5.1. Inselbildung effects become particularly important when small grid-to-cathode spacings are used and when the ratio of grid pitch to grid-to-cathode spacing is large (of the order of 1 or greater).

In Chapter 6 it is shown that high transconductance is needed for high gain in an amplifier stage. Let us therefore proceed to examine what factors affect the transconductance of a tube. Clearly, the transconductance is directly proportional to the cathode area A. An expression for the transconductance can be obtained by differentiating Equation (5.2-7) with

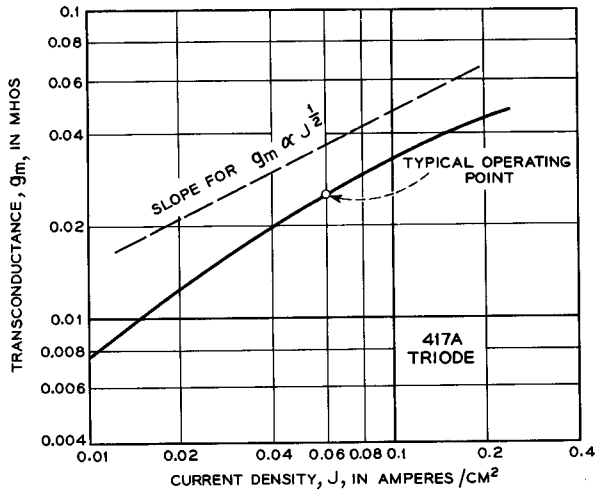

FIG. 5.2-6 Transconductance vs. cathode current density for the 417A triode.

respect to V_{go}. Thus

$$g_m = \frac{\partial I_{ao}}{\partial V_{go}} = Cn\left(V_{go} + \frac{V_{ao}}{\mu}\right)^{n-1} = Cn\left(\frac{I_{ao}}{C}\right)^{(n-1)/n} \tag{5.2-14}$$

Since both I_{ao} and C are proportional to the cathode area A, g_m is proportional to A, as we would expect. Furthermore $I_{ao} = JA$, where J is the current density drawn from the cathode. Consequently

$$g_m \propto J^{(n-1)/n} \tag{5.2-15}$$

For $n = 3/2$, $g_m \propto J^{1/3}$, and for $n = 2$, $g_m \propto J^{1/2}$. Figure 5.2-6 shows a plot of transconductance for the 417A triode vs. cathode current density. The normal operating point is marked with an X. In the neighborhood of this point it can be seen that g_m is approximately proportional to $J^{1/2}$, whereas at lower current densities g_m is proportional to a higher power of J.

The transconductance of a grid-controlled tube also increases as the distance between the grid and cathode is decreased, except at very small grid-to-cathode spacings, where Inselbildung effects become important. Figure 5.2-7 shows values of $g_m/J^{1/2}A$ vs. d_{cg} for several Western Electric tubes with small grid-to-cathode spacings and for a current density of 0.02 amp/cm². For most of these tubes, g_m is approximately proportional to $J^{1/2}$ at cathode current densities in the neighborhood of 0.02 amp/cm². The points appear to be distributed about a line with slope -1, indicating that $g_m \propto 1/d_{cg}$.

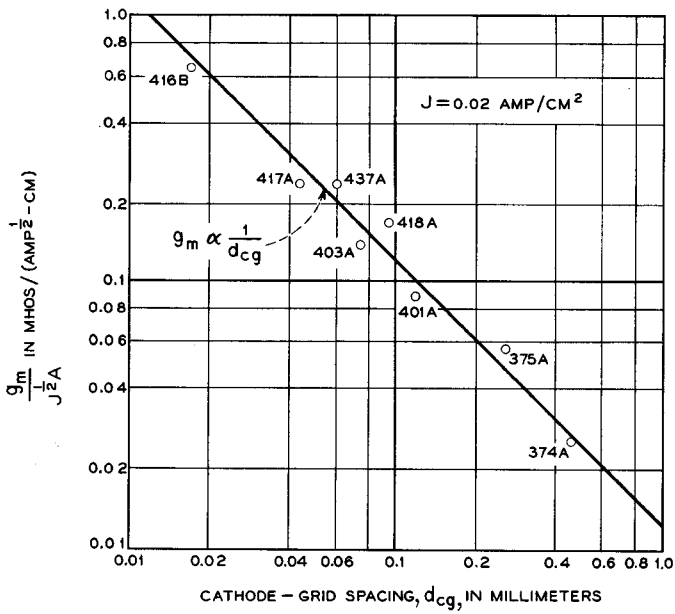

FIG. 5.2-7 Values of $G_m/J^{1/2}A$ plotted vs. d_{cg} for several Western Electric tubes.

A theoretical upper limit to the transconductance that can be obtained from unit area of the cathode is reached when the grid is located at the potential minimum and when the grid wires and pitch are sufficiently small that the potential over the plane of the minimum is equal to that of the grid. From the discussion given in Section 2.4, it follows that the anode current under these circumstances is

$$I_{ao} = J_o A \epsilon^{eV_{go}/kT} \tag{5.2-16}$$

where J_o is the cathode emission current density, A is the cathode area, and V_{go} is the grid bias voltage, *a negative number*. By differentiating this with respect to V_{go}, we obtain

$$g_m = \frac{\partial I_{ao}}{\partial V_{go}} = J_o A \frac{e}{kT} \epsilon^{eV_{go}/kT} = \frac{eI_{ao}}{kT} \tag{5.2-17}$$

Thus, in this theoretical upper limit of the transconductance of a grid-controlled tube, the transconductance is directly proportional to the current density $J = I_{ao}/A$ drawn from the cathode. (Note that J_o is the cathode emission current density, and J is the current density passing the potential minimum.) The ratio g_m/I_{ao} is equal to $11{,}600/T$ mhos/amp.

Figure 5.2-8 shows a plot of transconductance vs. grid-to-cathode spacing for the Western Electric 416B triode, described in Chapter 7 (Section 7.4). The transconductance reaches a maximum of 0.075 mho when the grid-to-cathode spacing is about 0.012 mm, and at still smaller spacings the trans-

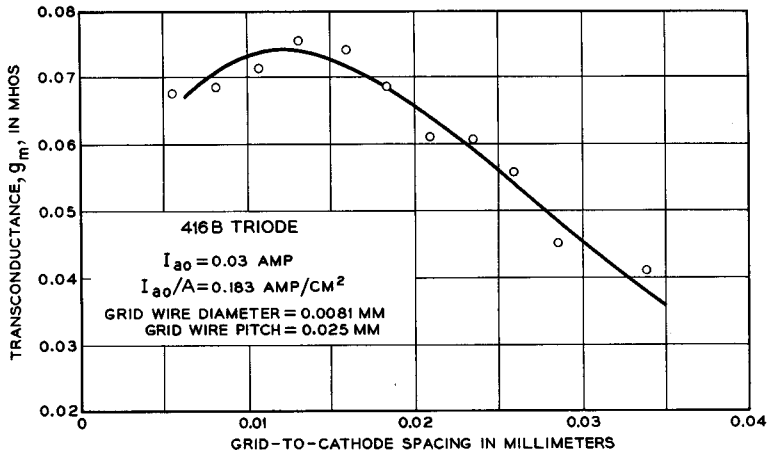

FIG. 5.2-8 Transconductance vs. grid-to-cathode spacing for the 416B triode described in Chapter 7.

conductance falls because of Inselbildung effects. The anode current for each of the experimental points was 0.03 amp, and the cathode temperature was close to 1025°K. Using these values in Equation (5.2-17), we find that the theoretical maximum transconductance is 0.34 mho. This is about 4.5 times the maximum observed transconductance, although the plane of the grid at maximum transconductance is approximately coincident with the plane of the potential minimum. It is probable that if a finer grid wire and smaller grid pitch were used, the theoretical maximum transconductance would be more nearly attained. However, the grid wire used in this tube is about as small as present technology permits.

In the 417A the grid is about three times as far from the cathode as the plane of the potential minimum. In consequence of this, the transconductance of the 417A is a still smaller fraction of the theoretical maximum. Typical values for the anode current and cathode temperature in the 417A are 0.027 amp and 1025°K. Substituting these values into Equation (5.2-17), we obtain a theoretical maximum transconductance of 0.31 mho, as compared with an actual transconductance of about 0.025 mho.

Since the plane of the potential minimum is always extremely close to the cathode, the control grid in most grid-controlled tubes is located well be-

yond the potential minimum. However in high-performance tubes, high transconductance is achieved by moving the grid closer to the potential minimum, generally at the expense of more difficult assembly procedures and higher cost.

Two more parameters that affect the transconductance are the grid-wire diameter and the grid pitch. At small grid-to-cathode spacings, the transconductance increases if both these quantities are reduced in such a manner that the screening fraction, or the ratio of the wire diameter to the pitch, is kept constant. An "open" grid structure, or small screening fraction, is usually desirable, since otherwise the beam current would be reduced, and the transconductance per unit area would be less. Often a pitch of between 4 and 10 times the grid-wire diameter is used. In many close-spaced, high-performance amplifier tubes the grid-wire diameter is chosen to be as small as is practicable from the standpoint of mechanical fabrication of the grid structure, and the grid pitch is then set to obtain maximum transconductance per unit area of the cathode, having due regard for limits imposed by the available cathode current density, the available electrode voltages, and the permissible electrode heat dissipation.

The following points will summarize our discussion about the transconductance of a triode:

1. The transconductance is directly proportional to the cathode area A.
2. The transconductance is proportional to a power of J which is of the order of 1/3 to 1/2 in practical cases.
3. The transconductance for a given J increases as the grid is moved closer to the cathode, until Inselbildung effects become important at very small grid-to-cathode spacings. When the grid is well beyond the potential minimum, the transconductance often varies approximately as $1/d_{cg}$.
4. At small grid-to-cathode spacings, the transconductance increases if the grid-wire diameter and pitch are reduced in such a manner that the screening fraction is kept constant.

The amplification factor is independent of the cathode area A, and it is almost independent of the cathode current density J (see Figure 5.2-2). Like the transconductance, the amplification factor increases if the grid-wire diameter and pitch are reduced in such a manner that the screening fraction remains constant. The amplification factor also increases as the grid-to-anode distance is increased.

Figure 5.2-9 shows the values of μ, g_m, and r_a for a number of commercial and Western Electric grid-controlled tubes used in low-power amplifier applications. The code numbers of the Western Electric tubes begin with the numbers 3 and 4. Values of μ for triodes typically vary from 5 to 100, values of g_m vary from 0.002 to 0.05 mho, and values of r_a vary from 10^2 to 10^4 ohms.

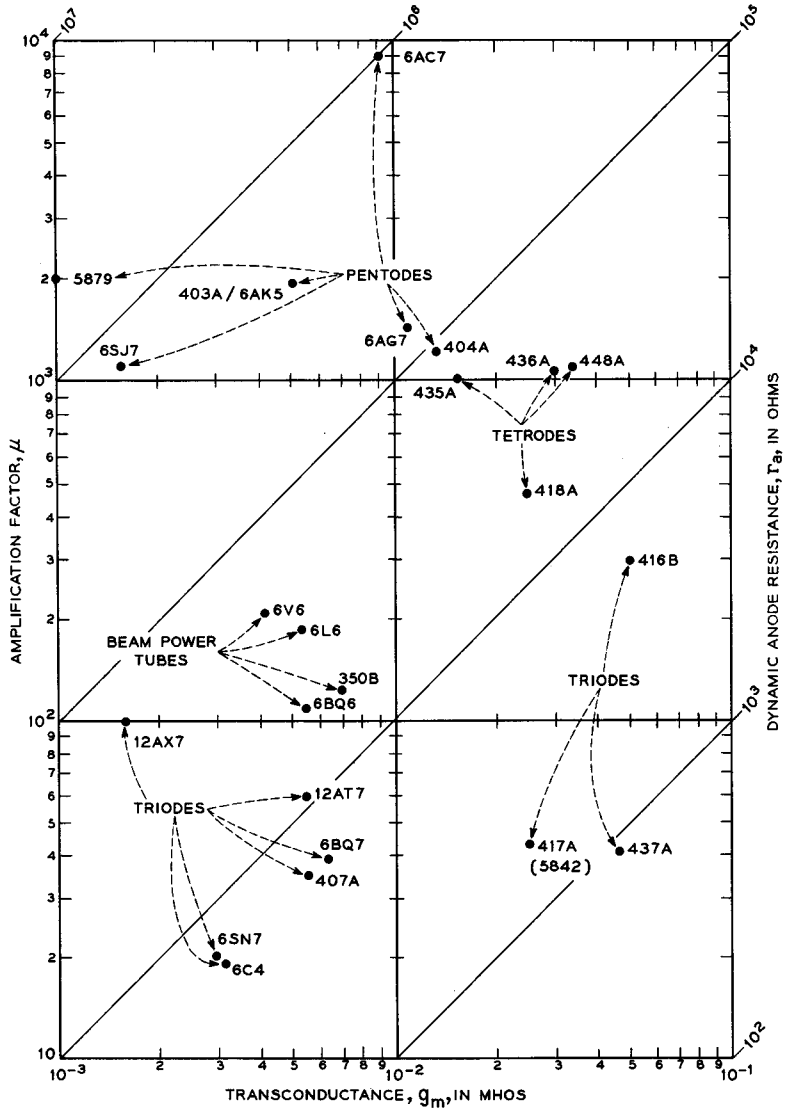

FIG. 5.2-9 The μ, g_m, and r_a of several commercial and Western Electric grid-controlled tubes used in low-power amplifier applications.

5.3 Tetrodes and Beam-Power Tubes

(a) *Tetrodes*

In the tetrode, a second grid, known as the screen grid, is inserted between the control grid and anode. The screen grid is usually of a coarser mesh than the control grid and is operated at a fixed positive voltage with respect to the cathode. It serves three principal functions:

1. It reduces the capacitance between the control grid and anode and hence the coupling between the input circuit and the output circuit.
2. In Chapter 6 we show that the input capacitance of a grounded-cathode triode amplifier stage is given by $C_{cg} + (1 + K)C_{ga}$, where C_{cg} is the cathode-to-grid capacitance, C_{ga} is the grid-to-anode capacitance, and K is the voltage gain of the stage. Since K may be a fairly large number, a small capacitance between the grid and anode may cause considerable shunting of the input signal at higher frequencies.[7] When a tetrode or pentode tube is used in a grounded-cathode amplifier stage, the shunting effect of the grid-to-anode capacitance is small, because C_{ga} is small, and consequently much higher input impedances are possible.
3. Over a range of positive anode voltages the current reaching the anode of a tetrode is determined almost entirely by the voltages applied to the control grid and screen grid and is nearly independent of the anode voltage. This means that the dynamic anode resistance of the tetrode is high, and this is an advantage in obtaining high gain per stage. In Chapter 6, the gain of a simple amplifier stage without feedback is shown to be $g_m R_L/(1 + R_L/r_a)$, where R_L is the load resistance and r_a is the dynamic anode resistance. (See Equation (6.3-7).) Clearly, high r_a is desirable where high gain is needed.

Figure 5.3-1 shows a cross-sectional view of the Western Electric 448A tetrode. Figure 5.3-1(c) shows a few of the grid wires and the relative spacings of the electrodes. Notice that the distance from the cathode to the screen grid in this tube is comparable with the distance from the cathode to the anode in the 417A. (See Figure 5.1-1 for comparison.) The 448A is used in a multistage amplifier which amplifies signals ranging in frequency from 58 to 90 Mc.

---

[7]Certain grounded-cathode triode circuits provide for "neutralization" of the grid-to-anode capacitance (Reference 5.4, p. 468), and much higher input impedances can be obtained. However, these circuits usually require careful adjustment of the circuit components in each stage if nearly complete neutralization is to be obtained. The grounded-grid circuit shown in Figure 6.3-5 has a much smaller capacitance between the anode and input circuit because the grid acts as an electrostatic shield. However, this circuit has a relatively low input impedance, of the order of $1/g_m$ in parallel with R_K. See Section 6.3.

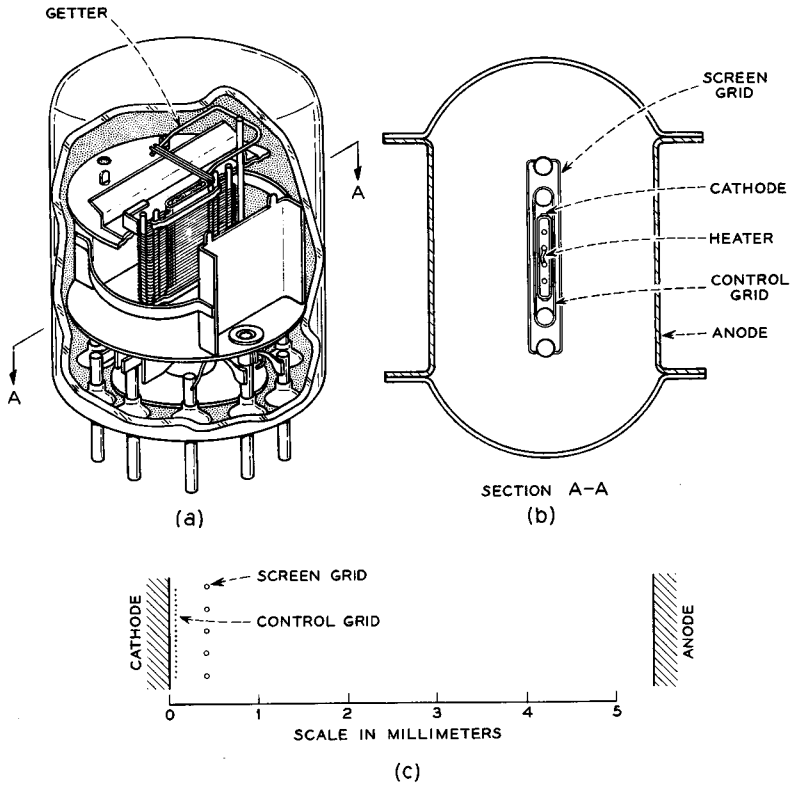

FIG. 5.3-1 The construction of the Western Electric 448A tetrode. The overall height of the tube is 4.8 cm.

The cathode of the 448A is a flattened nickel sleeve with a "double-carbonate" oxide coating. The control-grid wires are made of tungsten which is gold plated to raise its work function and reduce grid emission. The screen grid is also made of tungsten, but the wires are coated with fine carbon particles to increase heat radiation and reduce the operating temperature of the wires. The anode is made of carbonized nickel. The carbonizing increases the heat radiation from the outer surface and reduces the anode operating temperature. It also reduces secondary-electron emission from the anode.

Figure 5.3-2 shows the characteristic curves for the 448A. The screen-grid voltage is indicated by V_{sgo}. Notice that the grid characteristics with $V_{ao} = V_{sgo}$ are quite similar to the grid characteristics for a triode. The anode characteristics show that I_{ao} is nearly independent of V_{ao} over a

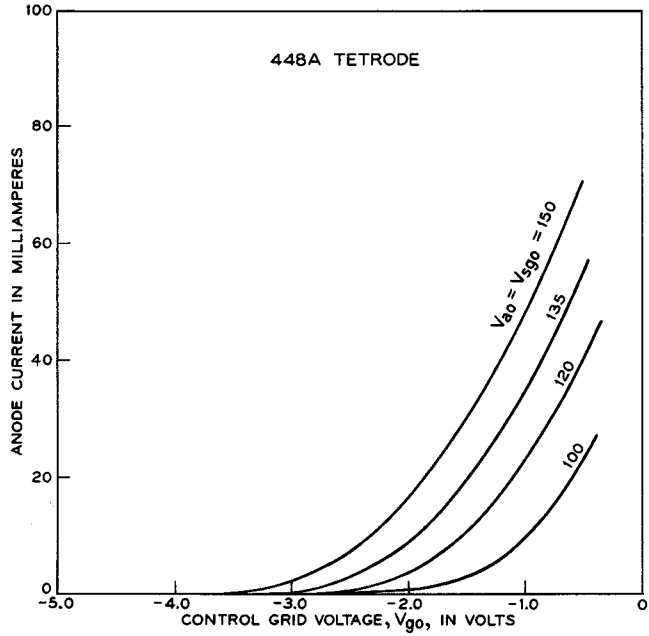

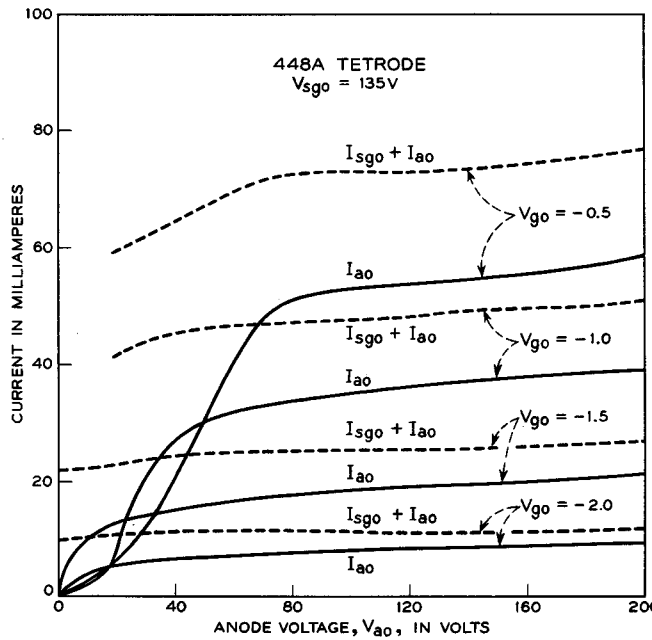

FIG. 5.3-2 The characteristic curves for the 448A tetrode.

range of positive anode voltages extending from well below screen-grid voltage to +200 volts or higher. Typical operating conditions for the 448A are given in Table 5.2-1.

Figure 5.3-1 shows that there is a large spacing between the screen grid and anode in the 448A. This serves two purposes:

1. With a large spacing, space charge between the screen grid and anode depresses the potential in the interelectrode space so that secondary electrons emitted from the anode are prevented from reaching the screen grid, and secondary electrons from the screen grid are prevented from reaching the anode. Without the potential depression, the current flowing in the anode circuit would be highly dependent on the relative voltages applied to the screen grid and anode, and the performance of the tube in an amplifier circuit would be seriously limited.
2. The large screen-anode spacing also reduces the output capacitance of the tube. The output capacitance is the capacitance between the anode and all other electrodes except the control grid. In Chapter 6 we shall find that a small output capacitance is desirable for tubes used in high-gain, broadband amplifiers.

Let us now look more closely at the potential between the screen grid and anode in the 448A. If we assume that the electron motion is normal to the plane of the electrodes and if edge effects are neglected, the potential between the screen grid and anode satisfies the one-dimensional form of Poisson's Equation,

$$\frac{d^2V}{dx^2} = -\frac{\rho}{\varepsilon_o} = -\frac{J}{\varepsilon_o\sqrt{2\eta V}} \tag{5.3-1}$$

where J is the beam current density passing through the screen grid, and x is the coordinate of the point at which V is determined. The potential V is measured relative to cathode potential, and the coordinate x is measured in the direction normal to the electrodes. Solutions of this equation covering four ranges of anode voltages V_{ao} are given in a paper by Fay, Samuel, and Shockley.[8] Figure 5.3-3 shows plots of these solutions for conditions which apply to the screen-anode space of the 448A. The four solutions of Fay, Samuel, and Shockley are described under separate headings below:

Solution A. $V_{ao} < 0$. In this case the potential decreases monotonically from the screen grid to the anode, but the shape of the potential is modified by the presence of space charge in the interelectrode space. At the point where the potential becomes negative, essentially all the electrons reverse

[8]Reference 5.5.

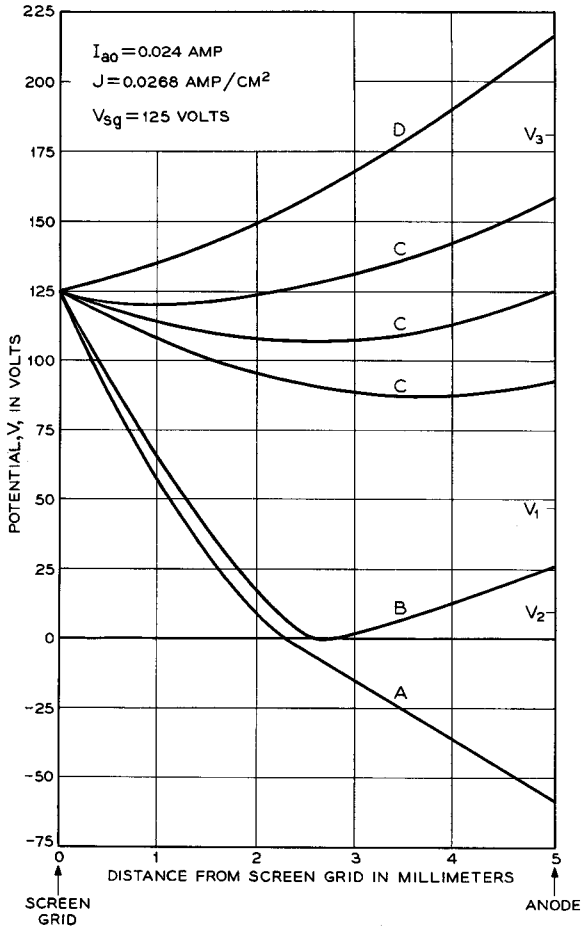

FIG. 5.3-3 Solutions of Equation (5.3-1) for a screen-grid voltage of 125 volts, a screen grid-anode spacing of 5 mm, and a beam current density of 0.0268 amp/cm². These are approximately the conditions that apply in the screen grid-anode space of the 448A tetrode under normal operating conditions.

the direction of their velocity and return to the screen grid. There is no space charge beyond this point. The anode current for this solution is, of course, zero.

Solution B. $0 \leq V_{ao} \leq V_1$. Here the anode voltage is positive, but a "virtual cathode" with potential $V = 0$ exists between the screen grid and anode. Since the electrons are emitted from the true cathode with a range

of velocities, the faster electrons pass the virtual cathode and reach the anode, while the remaining electrons reverse the direction of their velocity at the virtual cathode and return to the screen grid. The fraction of electrons passing the virtual cathode is determined by the applied anode voltage. When $V_{ao} = 0$, essentially all the electrons are returned to the screen grid. As V_{ao} is increased from zero, the fraction of electrons passing the virtual cathode increases until at some voltage V_1, all the electrons pass the virtual cathode, and the potential distribution suddenly changes to that of Solution C described below. (Note that $0 \leq V_{ao} \leq V_1$ is a necessary but not sufficient condition for Solution B to prevail, as discussed below.)

Solution C. $V_2 \leq V_{ao} \leq V_3$. Here the anode voltage is positive, and space charge between the electrodes depresses the potential in the interelectrode space so that there is a plane of minimum potential at some point between the electrodes. The potential at the minimum is greater than zero and less than either the screen or anode potential. All the electrons passing through the screen grid reach the anode when this solution prevails.

If the anode voltage is increased from zero through the voltage V_1, the potential distribution changes abruptly from the "virtual-cathode" distribution of Solution B to the "potential-minimum" distribution of Solution C. If the anode voltage is then lowered through the voltage V_1, Solution C prevails until some lower voltage V_2 is reached. Lowering the anode voltage still further causes the potential distribution to change abruptly to the virtual-cathode solution. This "hysteresis effect" in which there are two possible solutions to the potential distribution in the interelectrode space for anode voltages between V_1 and V_2 can be observed in a number of tetrode vacuum tubes. Of course, the anode current is less than the full beam current when Solution B prevails.

The position of the plane of minimum potential of Solution C moves closer to the screen grid as the anode voltage is increased. When $V_{ao} = V_3$, the plane of the potential minimum coincides with that of the screen grid.

Solution D. $V_{ao} > V_3$. Here the potential increases monotonically from the screen grid to the anode, and all the electrons reach the anode, as in Solution C.

In normal operation of the 448A, Solution C prevails. From Figure 5.3-3 it can be seen that, when $V_{sgo} = V_{ao} = 125$ volts, the potential minimum is about 18 volts below the screen and anode voltage. This potential depression greatly reduces the exchange of secondary electrons between the anode and the screen grid.

There are several sources of error involved in the use of Equation (5.3-1) and the solutions of Fay, Samuel, and Shockley to obtain the potential in the interelectrode space of a tube such as the 448A. First, edge effects are

neglected. Second, many of the electrons that pass close to the screen-grid wires as they enter the screen-anode space are deflected by strong local fields close to the screen-grid wires, so that the motion of these electrons is certainly not entirely in the x direction. Finally, from Figure 5.3-1(b) it is evident that the spacing between the screen grid and anode of the 448A is comparable with the linear dimensions of the cathode of the 448A, and consequently we would expect that the beam would spread as it travels between the screen grid and anode.

(*b*) *Beam-Power Tubes*

A second class of screen-grid tubes, known as beam-power tubes, also

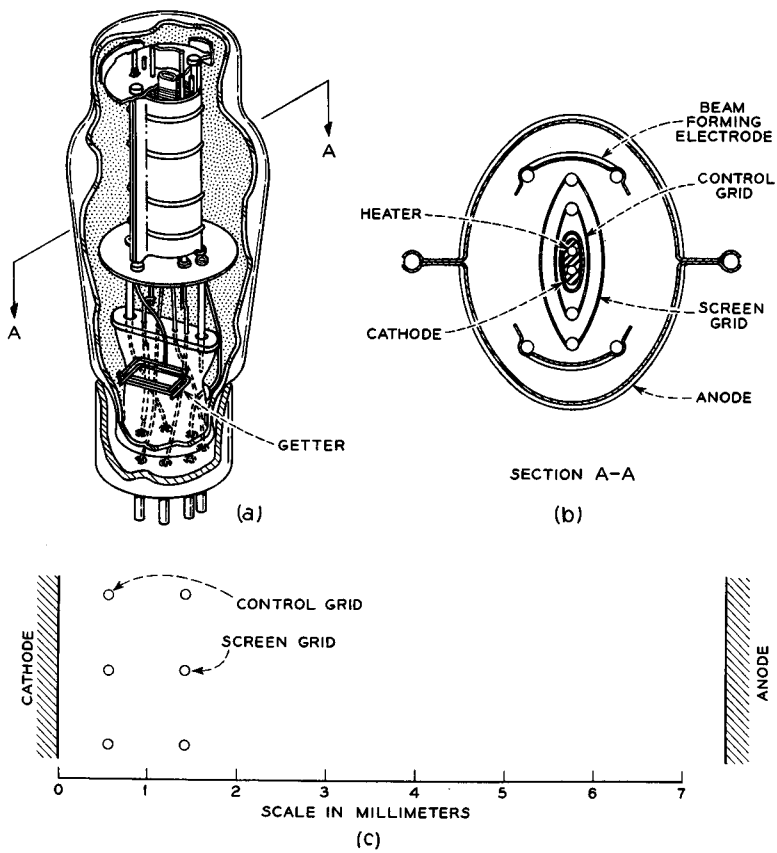

FIG. 5.3-4 The construction of the Western Electric 350B beam-power tube. The overall height of the tube is 14 cm.

makes use of a large screen-anode spacing so that the space charge of the electron beam depresses the potential between the screen grid and anode, and secondary electrons from one electrode are prevented from reaching the other. Figure 5.3-4 shows the construction of the Western Electric 350B beam-power tube. Notice that each screen-grid wire is directly opposite a control-grid wire. This construction greatly reduces the interception of the electron beam by the screen grid, since the negative bias on the control grid causes a "shadowing" of the screen-grid wires from the beam. In beam-power tubes an additional electrode, called a "beam-forming electrode," is located near the edge of the beam and held at cathode potential. This electrode also helps to depress the potential between the

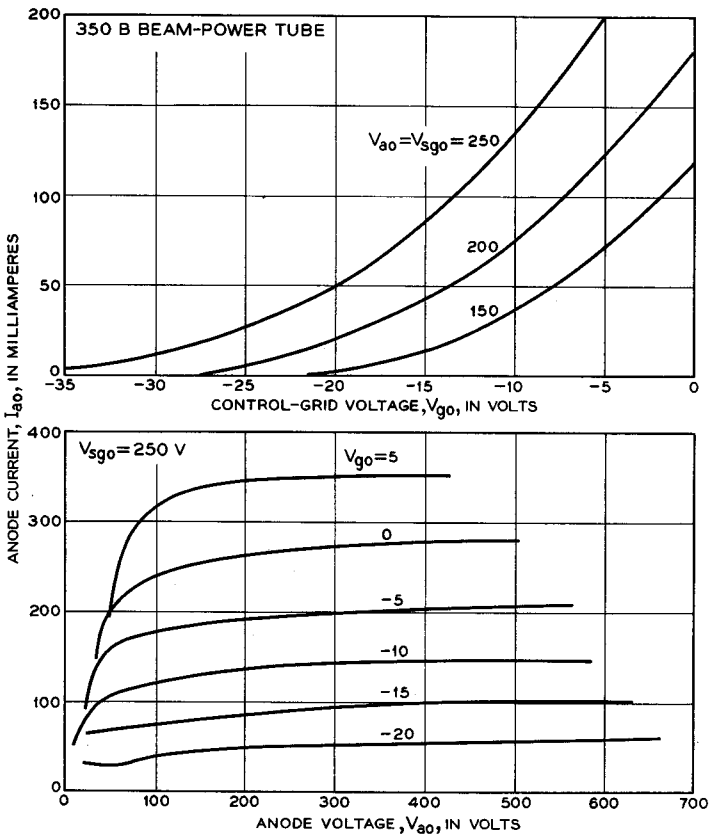

FIG. 5.3-5 The grid and anode characteristic curves for the Western Electric 350B beam-power tube.

screen grid and anode, but the principal cause of the potential depression in the region of the beam still arises from the space charge of the electron beam. The beam-forming electrode also prevents secondary electrons liberated from the anode from reaching the screen grid by means of paths outside the incident beam.

Typical operating conditions for the 350B are given in Table 5.2-1. The grid and anode characteristic curves for the 350B are shown in Figure 5.3-5. Note that the ratio of anode to screen-grid current is 8.9:1 for the 350B, whereas the same ratio for the 448A is 2.8:1.

The transconductance of a tetrode or beam-power tube is determined largely by the electrode geometry in the region between the cathode and the screen grid. However, it is reduced by the division of beam current between the screen grid and the anode. Often the interception of the beam current by the screen grid reduces the transconductance by 10 to 30 per cent over what it would be if the screen grid and anode were connected. The transconductance of the 350B is much lower than that of the 448A, principally because the 350B has a relatively large spacing between the cathode and control grid, and the distance between the control-grid wires is larger.

Figure 5.2-9 shows the μ, g_m, and r_a of a number of tetrodes and beam-power tubes. The transconductances of tetrodes and beam-power tubes fall in about the same range as those of triodes. However, the amplification factors of tetrodes are about an order of magnitude greater than those of triodes because of the shielding action of the screen grid.

5.4 Pentodes

Still another approach to the problem of eliminating the exchange of secondary electrons between the anode and the screen grid is that used in the pentode. Here a third grid, known as the suppressor grid, is inserted between the screen grid and anode. The suppressor grid is usually biased at cathode potential and therefore does not intercept any of the beam. Its pitch, or center-to-center wire spacing, is large, so that the potential at mid-point between grid wires is always well above cathode potential. In this way, most of the electrons that pass through the screen grid also pass through openings between suppressor-grid wires and travel on to strike the anode. However, the suppressor grid causes sufficient depression of the potential between the screen grid and the anode that it stops virtually all exchange of secondary electrons between these electrodes.

The pentode is by far the most widely used grid-controlled tube. Its advantages include high gain per stage and low grid-to-anode capacitance.

The construction of the Western Electric 403A pentode is illustrated in Figure 5.4-1. The electrode structure of this tube is similar to that of the 6AK5, a commercial code, and we shall refer to the tube as the 403A/6AK5 in subsequent discussion. The suppressor grid is located relatively close to

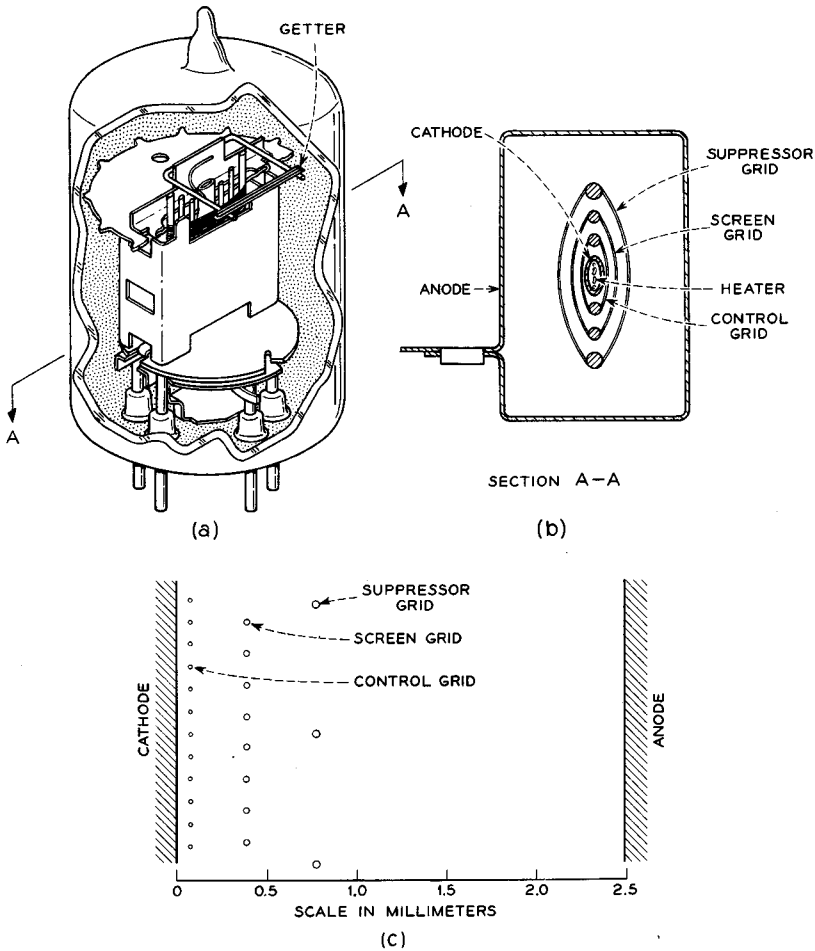

FIG. 5.4-1 The construction of the 403A/6AK5 pentode. The overall height of the tube is 4.4 cm.

the screen grid to reduce the output capacitance. Figure 5.4-2 shows the characteristic curves of the 403A/6AK5. Typical operating conditions are given in Table 5.2-1.

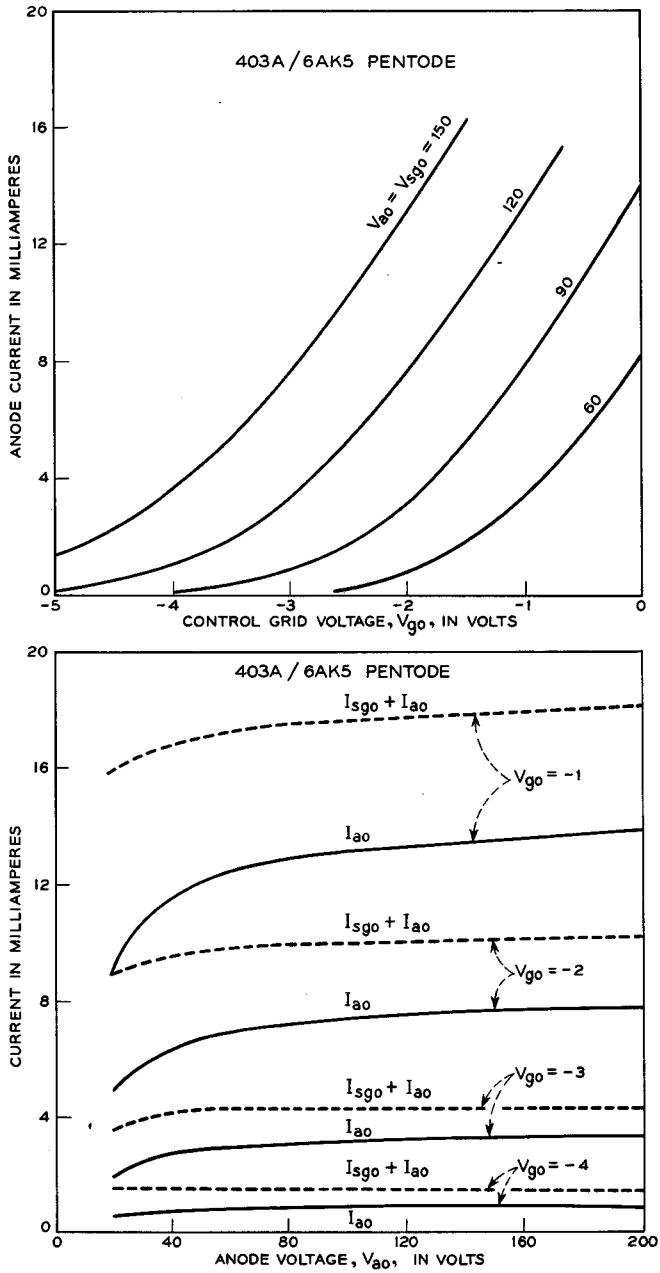

FIG. 5.4-2 The characteristic curves for the 403A/6AK5 pentode.

As in the tetrode, the transconductance of a pentode is determined largely by the electrode geometry in the region between the cathode and the screen grid and is reduced by the division of beam current between the screen grid and anode. Pentode transconductances are therefore of about the same magnitude as those of triodes and tetrodes. However, the amplification factor and dynamic anode resistance of a pentode tend to be even higher than for a tetrode because the suppressor grid provides added shielding between the anode and cathode. Pentode amplification factors usually lie between 10^3 and 10^4, whereas the dynamic anode resistance usually falls between 0.1 and a few megohms.

PROBLEMS

5.1 Show that the electrostatic amplification factor μ_{es} of a planar triode is given by

$$\mu_{es} = \frac{C_{cg}}{C_{ca}}$$

where C_{cg} is the capacitance between the grid wires and the cathode, but does not include the capacitance between the leads and electrode supports, and C_{ca} is the capacitance between the cathode and anode electrodes, but does not include the capacitance between the leads and electrode supports.

5.2 Equation (5.1-3) indicates that the electrostatic amplification factor μ_{es} depends upon the grid-wire diameter, the grid pitch, and the grid-to-anode spacing. However, it is nearly independent of the cathode-to-grid spacing d_{cg}, provided d_{cg} is large enough that the electric field at the surface of the cathode is uniform over the cathode surface. Can you explain qualitatively why μ_{es} should be nearly independent of d_{cg}?

5.3 An amplifier is constructed with two triodes in parallel. For the particular set of voltages applied to the electrodes, the dynamic characteristics of one tube are g_{m1}, r_{a1}, and μ_1, and those of the other tube are g_{m2}, r_{a2}, and μ_2. What are the g_m, r_a, and μ of the parallel combination?

5.4 A particular beam-power tube has a dynamic anode resistance of 200,000 ohms at a control-grid voltage of $V_{go} = V_1$, a screen-grid voltage $V_{sgo} = V_2$, and an anode voltage $V_{ao} = V_2$. If the screen grid is connected to the anode and the tube is operated as a triode, the dynamic anode resistance is 10,000 ohms with $V_{go} = V_1$ and $V_{ao} = V_{sgo} = V_2$. For a particular application the screen grid is used as the control electrode and the control grid is maintained at a constant bias voltage V_1. The screen grid and anode operating voltages are V_2. What is the transconductance of the tube using the screen grid as control electrode under these conditions? Assume that the screen-grid wires are ideally shielded behind the control-grid wires so that there is essentially zero current intercepted by the screen grid. Note that, for incremental variations in the applied potentials, the incremental change in anode current can be expressed as

$$dI_{ao} = \frac{\partial I_{ao}}{\partial V_{go}} dV_{go} + \frac{\partial I_{ao}}{\partial V_{sgo}} dV_{sgo} + \frac{\partial I_{ao}}{\partial V_{ao}} dV_{ao}$$

REFERENCES

Three general references covering the principles and design of grid-controlled tubes are:

5a. K. R. Spangenberg, *Vacuum Tubes*, Chapters 7 to 11, McGraw-Hill Book Co., Inc., New York, 1948.

5b. W. G. Dow, *Fundamentals of Engineering Electronics*, 2nd Ed., Chapters 4 to 6, John Wiley and Son, Inc., New York, 1952.

5c. A. H. W. Beck, *Thermionic Valves*, Chapters 9 to 11, Cambridge University Press, Cambridge, England, 1953.

Other references covering specific topics referred to in this chapter are:

5.1 W. R. Bennett and L. C. Peterson, *Bell System Tech. J.* **28**, 303, 1949.

5.2 I. Langmuir and K. T. Compton, *Rev. Modern Phys.* **3**, 241, 1931.

5.3 P.H.J.A. Kleynen, *Philips Res. Reports* **1**, 81, 1946.

5.4 F. E. Terman, *Radio Engineer's Handbook*, McGraw-Hill Book Co., Inc., New York, 1943.

5.5 C. E. Fay, A. L. Samuel, W. Shockley, *Bell System Tech. J.* **17**, 49, 1938.